15 Myocardial Viability

Shahram Bonyadlou and Sindu Sheth

FDG Viability Scintigraphy

Introduction

Among all methodologies in the diagnosis of hibernating myocardium, ^{18}F-FDG PET has remained a significant diagnostic tool. In combination with myocardial perfusion scintigraphy, FDG PEt allows differentiation between scar and viable myocardium and extent of disease with remarkable certainty. This leads to appropriate patient selection for invasive revascularization procedure. FDG PET has also been helpful in patients with diagnosis of cardiac sarcoidosis and evaluation of patients with cardiomyopathy for resynchronization therapy or who are being considered for revascularization or heart transplant.

Overview

Normal myocardium utilizes free fatty acids or glucose to generate energy. Under aerobic conditions, free fatty acids are the main sources of energy unless there is circulating insulin to facilitate glucose consumption. During severe ischemia (viable), myocardium switches to anaerobic metabolism, utilizing glucose as the sole source of energy. Therefore, ^{18}F-FDG PET will detect an ischemic myocardium (hibernating).

Technique

Perhaps the most important factor in obtaining a quality image is patient preparation. The following protocol has been successfully implemented in our institution.

P.S. Conti, A. Kaushik (eds.), *PET-CT*, DOI 10.1007/978-1-4419-5811-2_15

[^{18}F]-FDG Cardiac Viability Imaging Protocol

Scheduling Considerations

A resting myocardial perfusion study must be obtained within the month prior to the PET scan, and there must be no change in the patient's clinical status between the perfusion scan and the viability scan.

Patient Preparation

Obtain patient history including allergies, risk factor, diabetes, medication, known cardiovascular therapy, and prior cardiovascular tests (echocardiography, SPECT, MRI, or invasive coronary angiography).

The patient must have a resting myocardial perfusion scintigraphy (thallium, Myoview/MIBI, or rubidium) prior to viability scintigraphy.

Glucose management for diabetic cardiac patients is individually reviewed by the nuclear medicine physician, radiologist, or nurse. However, generally diabetic patients are instructed to eat a high-protein/low-carbohydrate dinner the evening before the scan. Diabetics using oral hypoglycemic agents are asked to take the normal dose of medication and no breakfast the day of the study (early morning schedule).

If the study must be scheduled for the afternoon, the patient is instructed to eat a high-protein/low-carbohydrate light breakfast, take a full dose of morning hypoglycemic agent or insulin, and abstain from eating lunch.

Tube feeding and intravenous dextrose solution must be placed on hold 3–6 h prior to study. Nicotine and caffeine consumption must be held 24 h prior to viability scintigraphy.

Radiopharmaceutical Dosage

Adult dose: ^{18}F-FDG 10–20 mCi IV or 0.22 mCi/kg.

Pediatric dose: adjusted pediatric dose schedule = (0.14–0.21 mCi) [^{18}F] IV not to exceed 10 mCi.

Clinical Imaging Procedure

1. Height, weight, and blood glucose are measured. An intravenous catheter is placed and left throughout the study.
2. Cardiac monitoring.
3. Obtain serum fasting blood glucose (BG).
4. Glucose is administered PO.
5. **Nondiabetic**

Oral glucose loading:

(a)	If BG < or = 150 mg/dl	50 g oral glucose + regular insulin 3 units IV
(b)	If BG 151–300 mg/dl	regular insulin 5 units IV
(c)	If BG 301–400 mg/dl	regular insulin 7 units IV
(d)	If BG > 400 mg/dl	consult physician

IV glucose loading (if unable to load PO): see below

FDG administration: After glucose load and sliding scale insulin injections, administer F-18 FDG at least **45 min** after glucose loading and when BG < or = 150 mg/dl.

6. **Diabetic**
   Oral glucose loading:

(a)	If BG < or = 150 mg/dl	25 g oral glucose
(b)	If BG 151–180 mg/dl	regular insulin 5 units IV
(c)	If BG 181–200 mg/dl	regular insulin 7 units IV
(d)	If BG 201–300 mg/dl	regular insulin 12 units IV
(e)	If BG > 400 mg/dl	consult physician

IV glucose loading (if unable to load PO): see below

FDG administration: After glucose load and sliding scale insulin injections, administer F-18 FDG at least **60 min** after glucose loading and when BG ≤ 150 mg/dl.

7. 15 min following administration of oral glucose load, obtain blood glucose level and repeat every 15 min and administer IV regular insulin as per above protocol.
8. Residual activity in the syringe and tubing is assayed and used to determine the actual administered activity.
9. Following uptake period, the patient is transferred to the imaging table.
10. The patient is positioned with their arms up (preferred) or at their side. Scout images are acquired to determine position and whether there is adequate FDG uptake in the myocardium.
11. Routine cardiac imaging should not begin sooner than 40 min post injection. If myocardial uptake is still negligible after 40 min, the nuclear medicine physician must be notified.
12. The blood glucose level must be >80 mg/dl prior to discharge. The patient will be observed for signs of hypoglycemia during the entire procedure while in the PET center. If blood sugar is ever less than 80 mg/dl after insulin administration, start D5W @ 100 cm^3/h IV. Recheck blood glucose in 15 min.

IV Glucose Loading Instruction

(a) If the fasting glucose level is <150 mg/dl, 25 g dextrose-50 is given intravenously. (20–25 mg of hydrocortisone should be added to the dextrose-50 prior to injection to reduce the irritation of the veins.)
(b) For fasting glucose levels between 150 and 200, administer 12.5 g dextrose-50 dose.
(c) For fasting glucose levels >200, implement sliding scale insulin to lower the blood sugar using the following formula:

$$\text{Units of regular insulin IV} = \frac{\text{BS} - 50}{25}.$$

Note: Up to 10 units IV per dose (i.e., no single dose greater than 10 units of regular insulin should be given).

(d) After each insulin dose, blood sugar should be checked 15 min after the dose is given.
(e) If blood sugar is ever less than 80 mg/dl after insulin administration, start D5W @ 100 cm^3/h IV. Recheck blood glucose in 15 min.
(f) If hypoglycemia occurs (patient becomes diaphoretic, tachycardic, disoriented, etc.), give dextrose-50, 1 ampule IV, and start D5W @ 100 cm^3/h IV.
(g) Insulin is administered by physician or PET nurse only.
(h) If the blood sugar is = or < 150 mg/dl following sliding scale protocol, FDG can be injected.
(i) If the blood sugar remains >150 mg/dl, continue sliding scale insulin formula prior to injection of the FDG.

Case 15.1 History

A 57-year-old male with known history of coronary artery disease, status post CABG, was referred for myocardial viability.

Rows 1 and 3 (short-axis images) demonstrated a large area of perfusion abnormality at rest (SPECT myocardial perfusion scintigraphy—^{99m}Tc-tetrofosmin) involving the inferior left ventricular wall (Fig. 15.1). Rows 2 and 4 ^{18}F-FDG viability scintigraphy demonstrated a nonviable myocardium.

Top row (vertical axis) image resting SPECT myocardial perfusion scintigraphy (^{99m}Tc-tetrofosmin) (Fig. 15.2). Bottom row ^{18}F-FDG viability scintigraphy demonstrated no viable myocardium in the inferior wall.

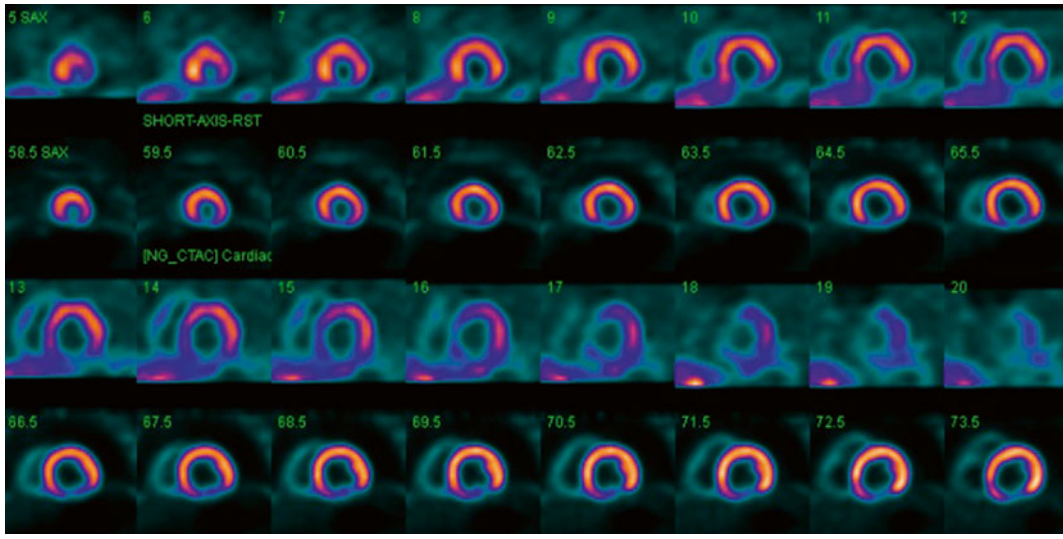

Fig. 15.1

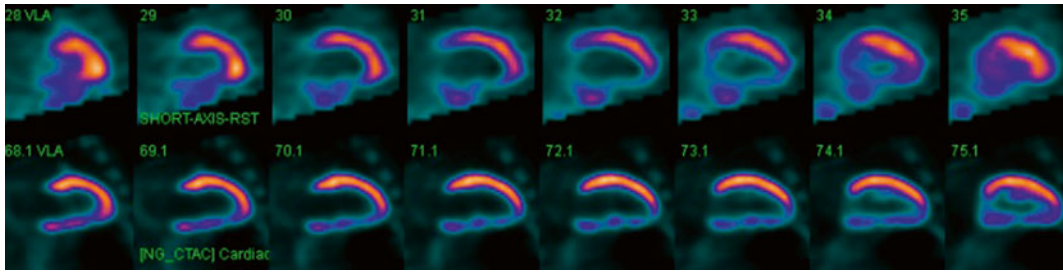

Fig. 15.2

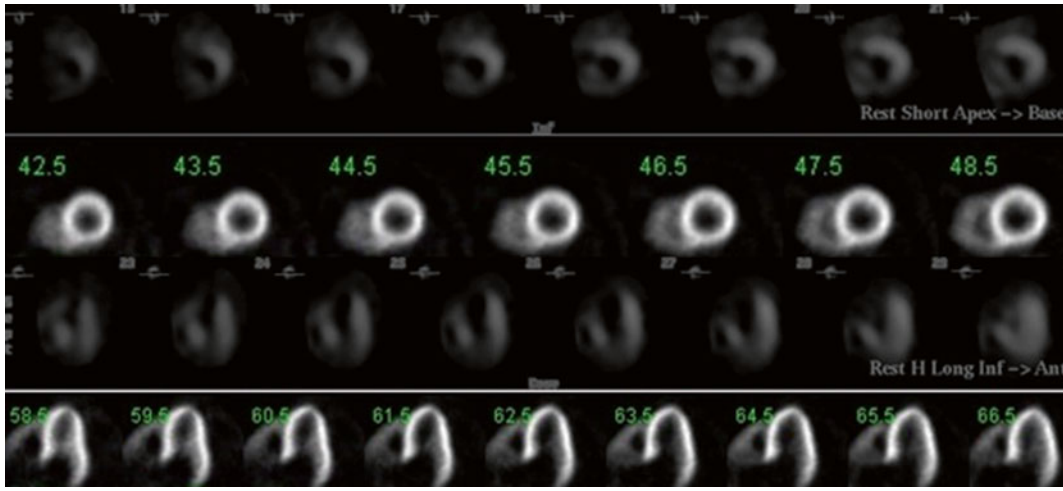

Fig. 15.3

Case 15.2 History

A 72-year-old male with known history of coronary artery disease, status post PTCA stent of RCA, was referred for evaluation of myocardial viability. Image 2 showed a moderate size perfusion abnormality involving inferoseptal left ventricular myocardium. This region demonstrated physiologic activity on FDG scintigraphy, indicating a viable myocardium.

Rows 1 and 3 demonstrated a large area of perfusion abnormality at rest SPECT myocardial perfusion scintigraphy (^{201}thallous chloride) (Fig. 15.3). Rows 2 and 4 demonstrated a viable myocardium on ^{18}F-FDG PET scintigraphy.

Artifacts Associated with PET-CT Myocardial Perfusion Scintigraphy

Misregistration of PET and CT Transmission Data

Misregistration of PET and transmission data is common in cardiac PET imaging, resulting in false interpretation. As a quality control measure, assessment of registration images of PET and CT must be performed routinely. This is important for processing PET data based on underlying soft tissue attenuation level. As a result, over- or undercorrection of PET data may occur.

Case 15.3

A 54-year-old male with hypertension and diabetes and abnormal ECG, complaining of chest pain of suspected ischemic origin (Fig. 15.4). Patient underwent routine rubidium-82 myocardial perfusion scintigraphy. Stress fusion images (PET rubidium-82 cardiac perfusion and CT transmission scan) demonstrate misregistration of the lateral wall of the left ventricle within low attenuating tissue of the lung parenchyma. The resting fusion images demonstrated appropriate registration.

Attenuation-corrected rubidium-82 cardiac perfusion PET demonstrates hypoactivity of the lateral wall at stress and normal activity at rest, most suspected for ischemia (Fig. 15.5).

Images demonstrate appropriate registration of rubidium-82 cardiac perfusion and transmission scans (manual correction was made) (Fig. 15.6). Note: Alignment must be made in 3-D format.

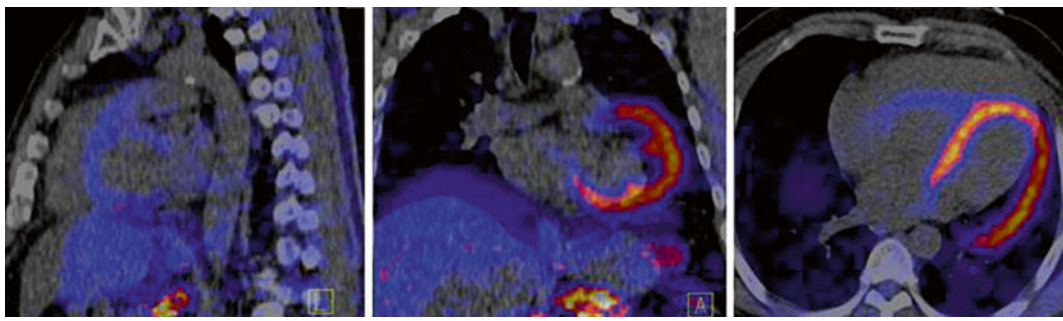

Fig. 15.4

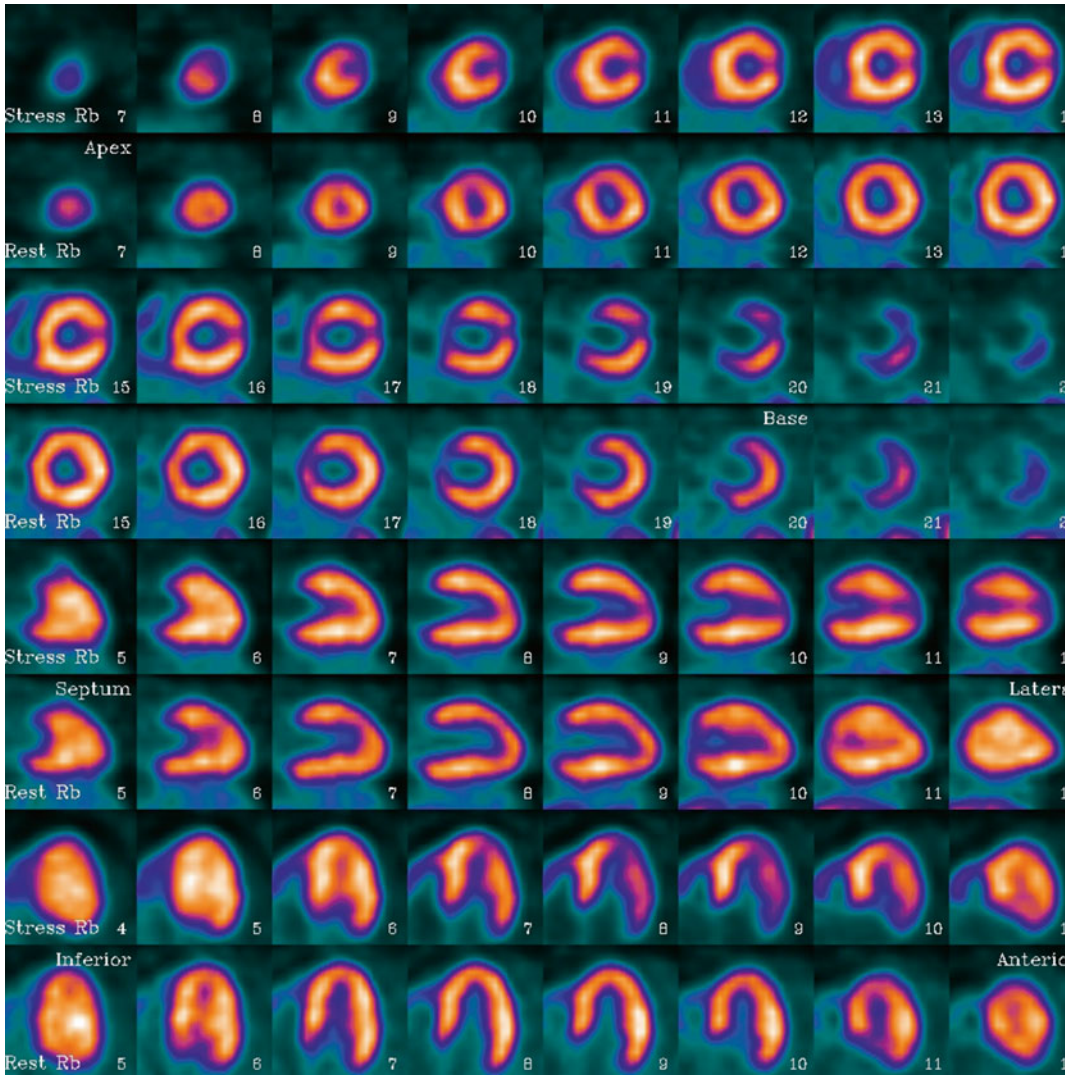

Fig. 15.5

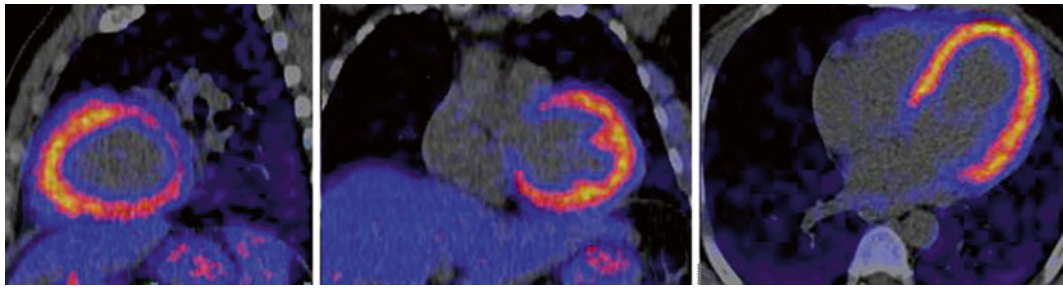

Fig. 15.6

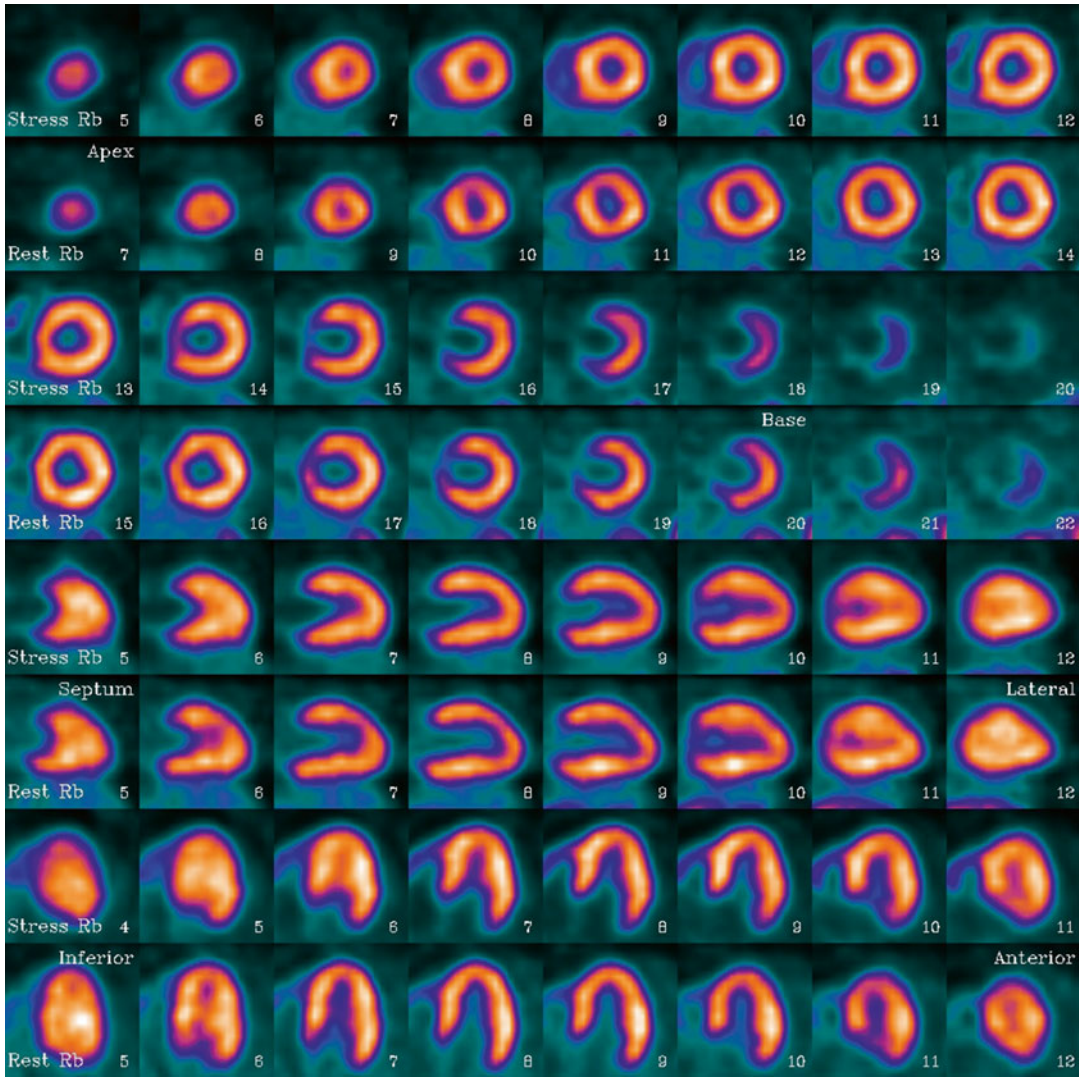

Fig. 15.7

Following correction of registration data, rubidium-82 cardiac perfusion images demonstrate resolution of hypoactivity of the lateral wall (Fig. 15.7).

Breast Attenuation Artifact

Although markedly reduced, attenuation associated with soft tissue of the breast must be excluded.

Case 15.4

Following images demonstrate hypoactivity of the anterior wall in a 64-year-old female with long-standing hypertension and hyperlipidemia, complaining of chest pain and shortness of breath. The anterior wall hypoactivity appears more pronounced at rest than stress (Figs. 15.8 and 15.9). Acquisition of gated data was at the time of peak stress, representing a true stress wall motion and wall thickening. Figures 15.10 and 15.11 demonstrate end-diastolic and end-systolic gated images, respectively. There is appropriate thickening of the anterior wall at end-systolic images, confirming attenuation artifact attributed to breast parenchyma.

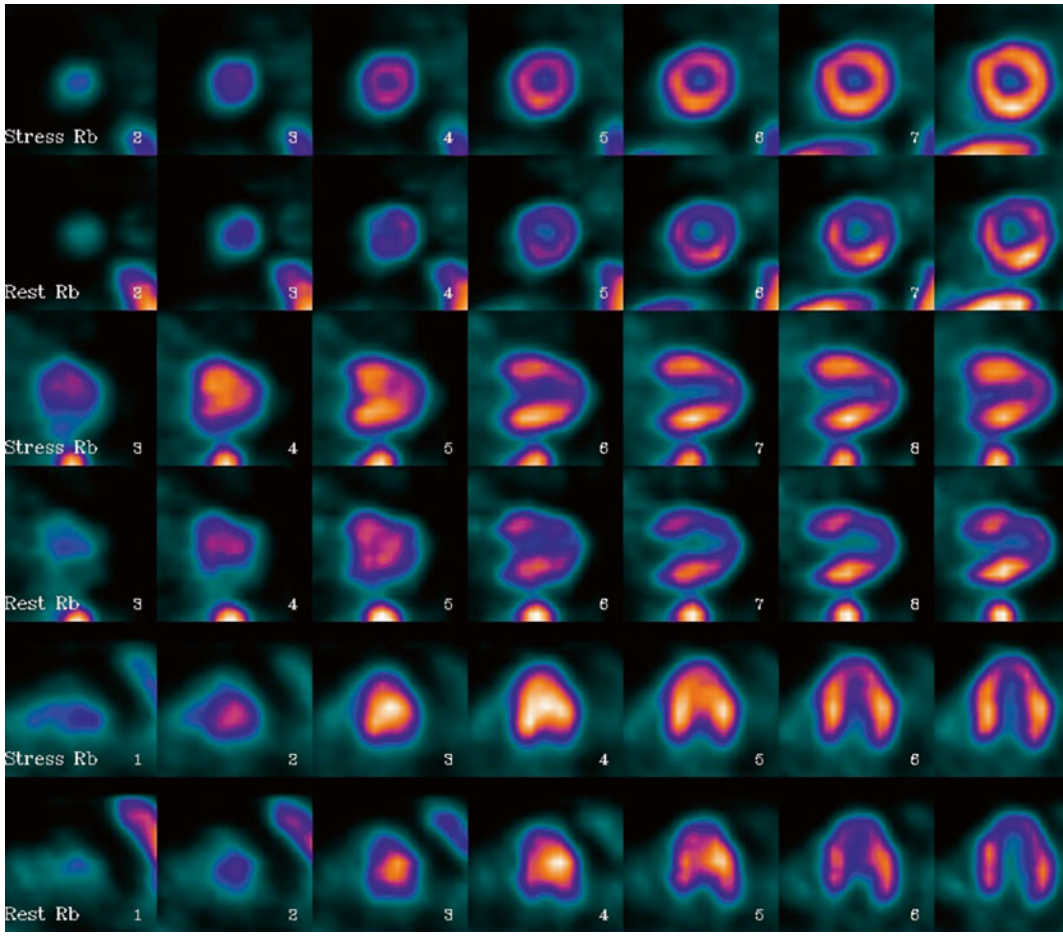

Fig. 15.8

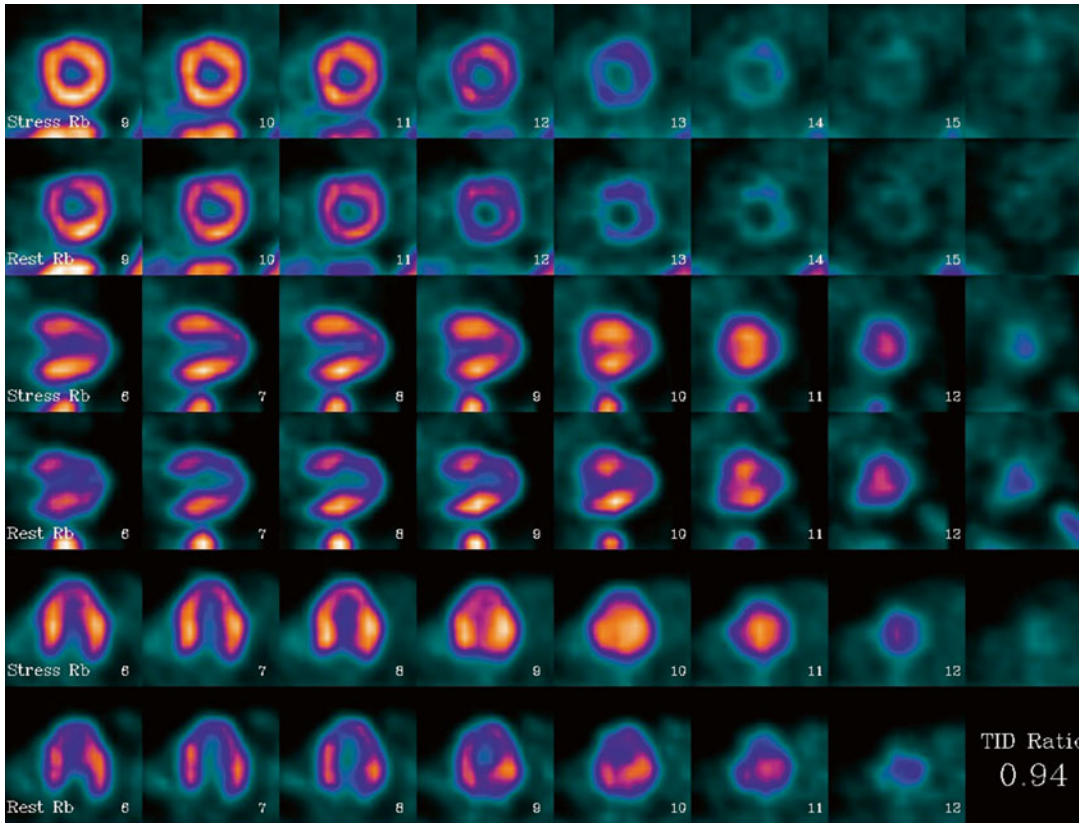

Fig. 15.9

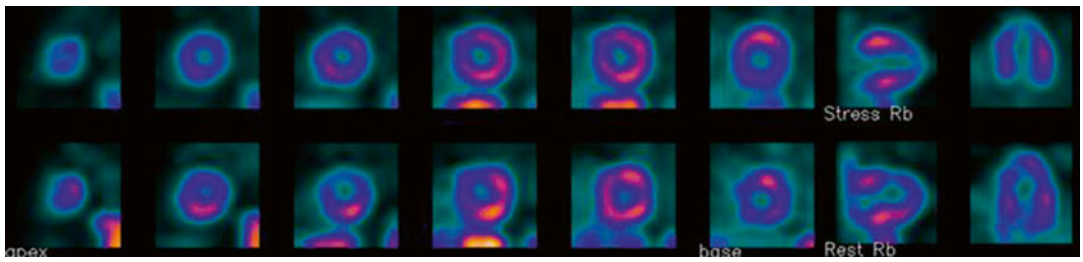

Fig. 15.10

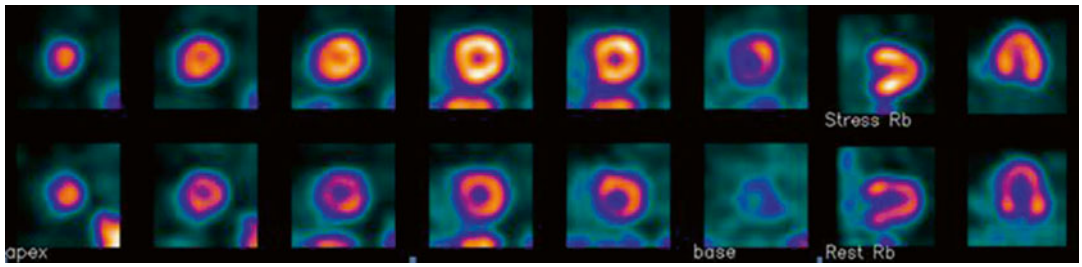

Fig. 15.11

Attenuation Attributed to Large Region of Interest

Whether automatic or manual, there would be an Region of Interest (ROI) drawn within processing matrix to normalize the left ventricular count profile. The field of view may or may not include noncardiac activities. This adversely affects the normalization process, therefore affecting myocardial activity.

Figures 15.12 and 15.13 demonstrate initial (automatic) placement of ROI that included the left ventricle as well as intense subdiaphragmatic activity. Normalization was based on the most active region within ROI. The stress images were normalized to left ventricular myocardial activity, whereas resting images were normalized to subdiaphragmatic activity (Fig. 15.13).

Figure 15.14 demonstrates manual correction of ROI only to the left ventricle. Note following correct placement of ROI, the resting left ventricular activity is appropriately normalized at rest (Fig. 15.15).

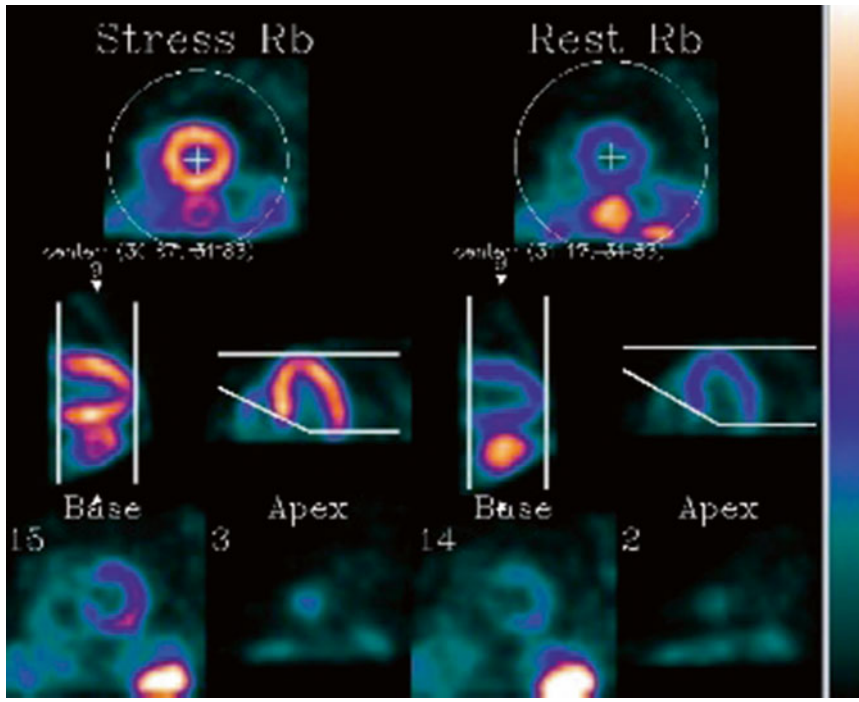

Fig. 15.12

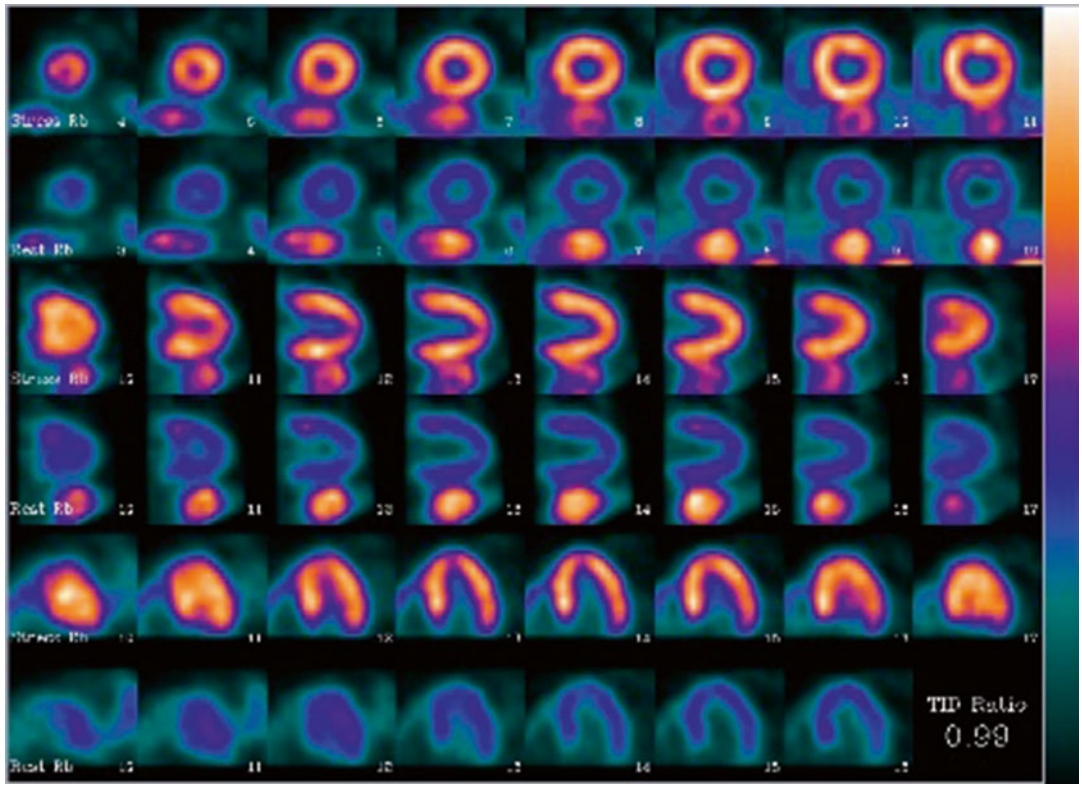

Fig. 15.13

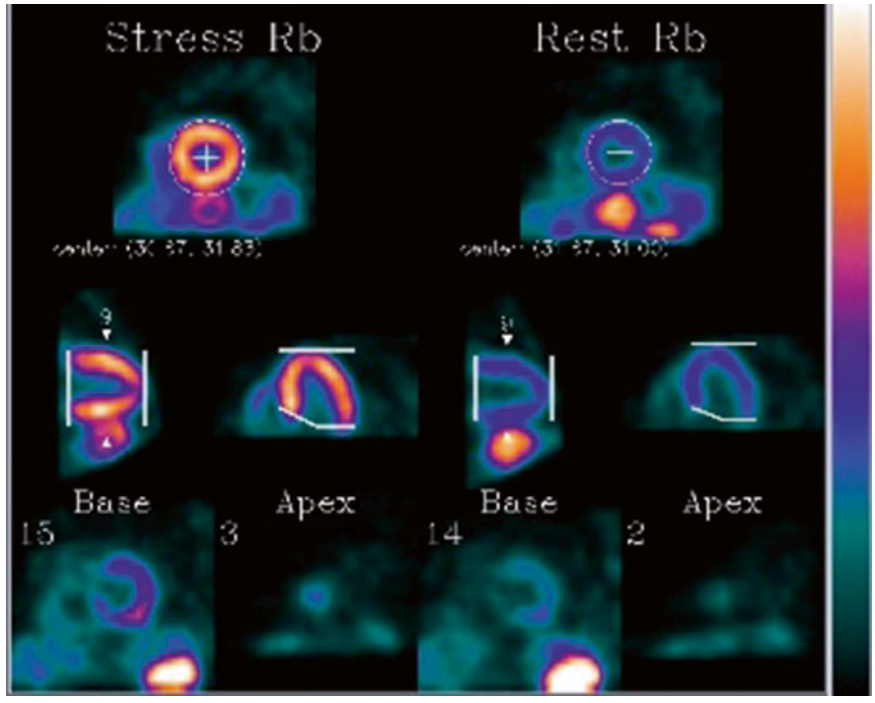

Fig. 15.14

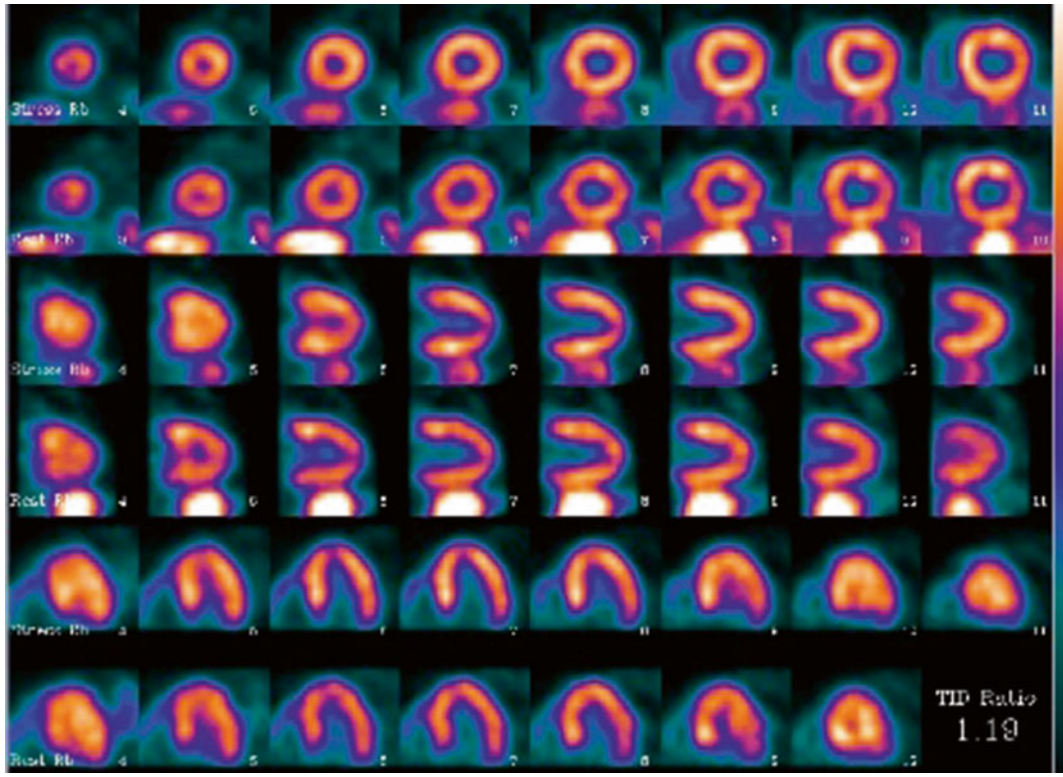

Fig. 15.15

Noncardiac Findings

1. PET
   (a) Chest: mediastinal, esophageal, pulmonary, skeletal, breast, thyroid, cervical, and subdiaphragmatic.

   Attention must be made to noncardiac activities during the evaluation process, similar to conventional SPECT scintigraphy as radiotracer activity may localize to pathological processes such as a tumor. Careful evaluation of raw data during quality control (registration assessment) process is a must.
2. CT
   (a) Nonmalignant: mediastinal, pulmonary, skeletal, esophageal, cervical, and nodal.
   (b) Malignant: primary and metastatic.

   Most PET myocardial scintigraphies are performed, using hybrid equipments (PET-CT). Quality of transmission CT scan images is poor secondary to low level of radiation (50–70 mAs) and acquisition during mild respiration. However, one must carefully examine the transmission CT dataset as it may reveal benign or malignant lesions.

Case 15.5

Transmission scan of rubidium myocardial perfusion scintigraphy (Fig. 15.16) demonstrates heterogeneous attenuation through liver parenchyma, highly suspicious of malignancy. Patient was referred for a FDG PET-CT scan for further clarification.

PET-CT scintigraphy (Fig. 15.17) demonstrated hypermetabolic activity associated with hypoattenuating liver lesions. Tissue sampling revealed metastatic disease from colon carcinoma.

Case 15.6

A 70-year-old male with hypertension, hyperlipidemia, and family history of coronary artery disease was being evaluated for chest discomfort of suspected ischemic origin. Axial CT transmission scan images demonstrated large hiatal hernia and vertebral body hemangioma (Fig. 15.18). Rubidium myocardial perfusion scintigraphy was unremarkable. No prior anatomical imaging was performed prior to rubidium scintigraphy. Patient's symptom was attributed to hiatal hernia and GERD. Subsequent management of GERD resulted in complete cessation of symptoms.

Case 15.7

A 55-year-old female with hypertension and family history of coronary artery disease was referred for assessment of coronary artery disease. Axial CT transmission images demonstrated large retrotracheal/mediastinal

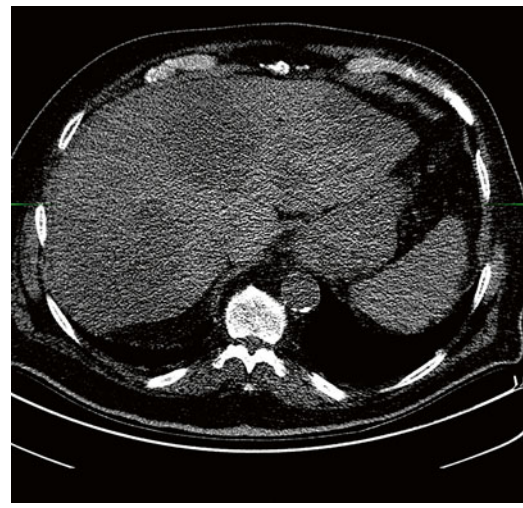

Fig. 15.16

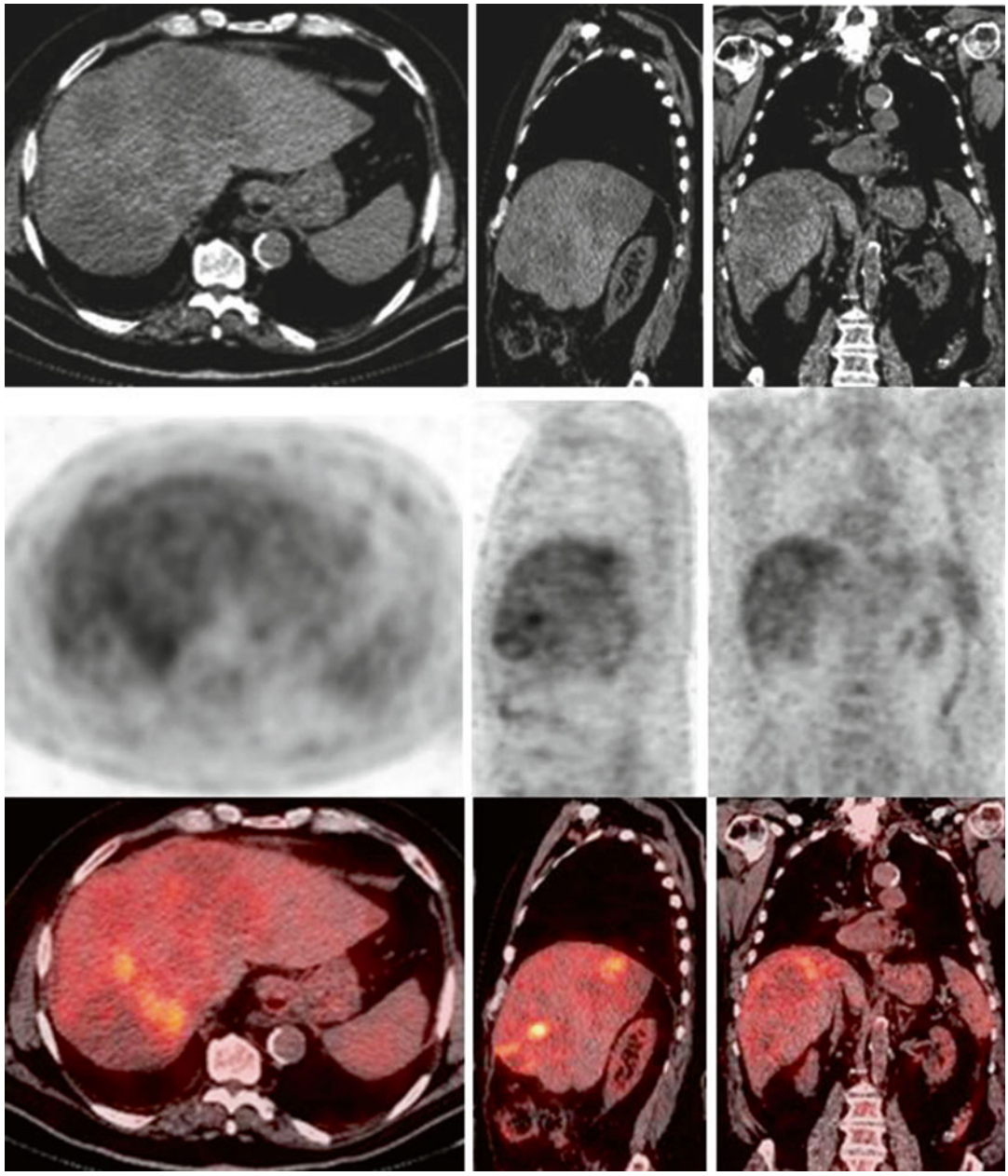

Fig. 15.17

mass that was worrisome for malignant etiology (Fig. 15.19). Further correlation with ^{18}F-FDG PET-CT scan identified the mass as mediastinal extension of a large goiter. Subsequent management of goiter resulted in resolution of chest pain.

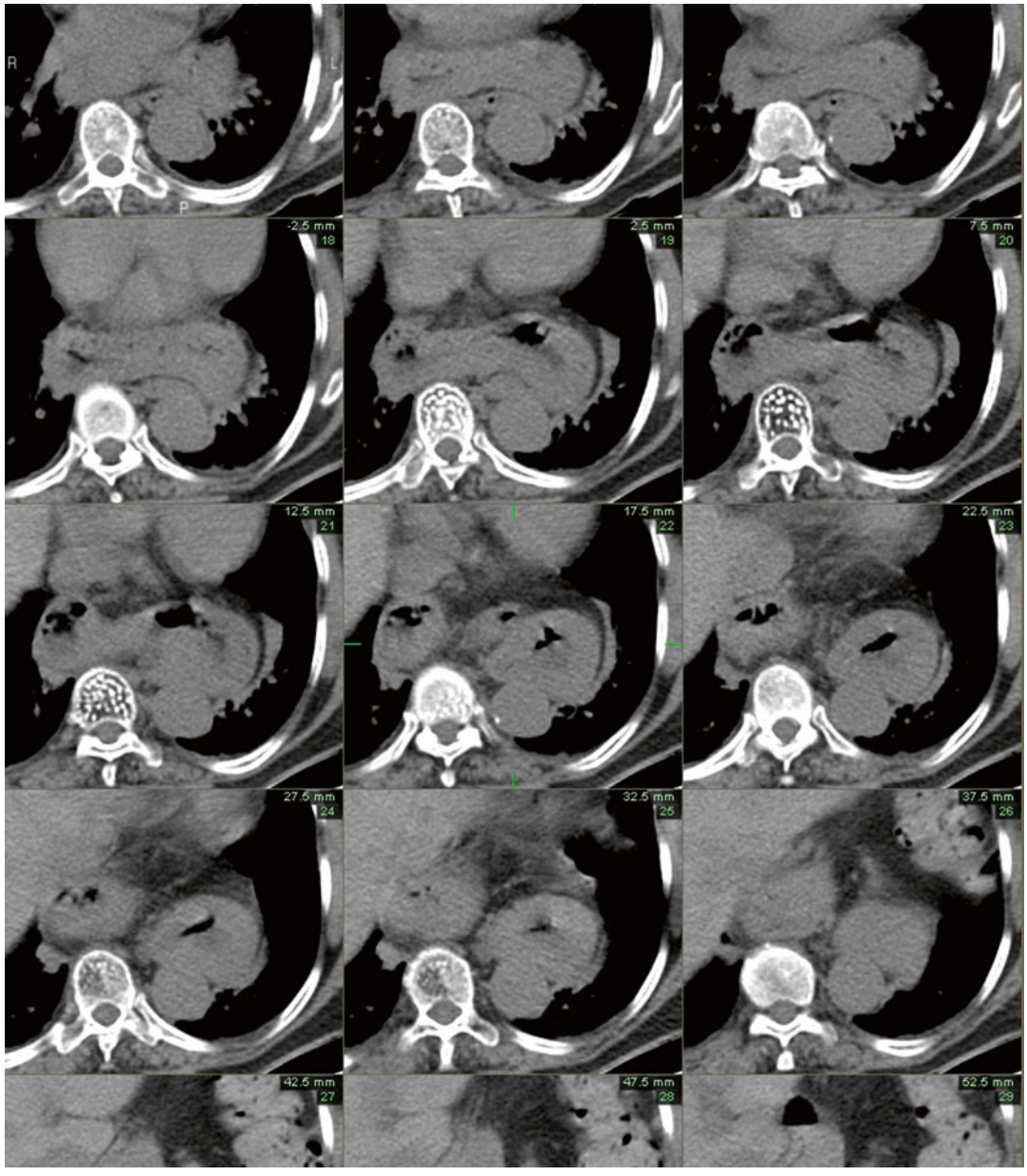
R
L
P
-2.5 mm
18
2.5 mm
19
7.5 mm
20
12.5 mm
21
17.5 mm
22
22.5 mm
23
27.5 mm
24
32.5 mm
25
37.5 mm
26
42.5 mm
27
47.5 mm
28
52.5 mm
29

Fig. 15.18

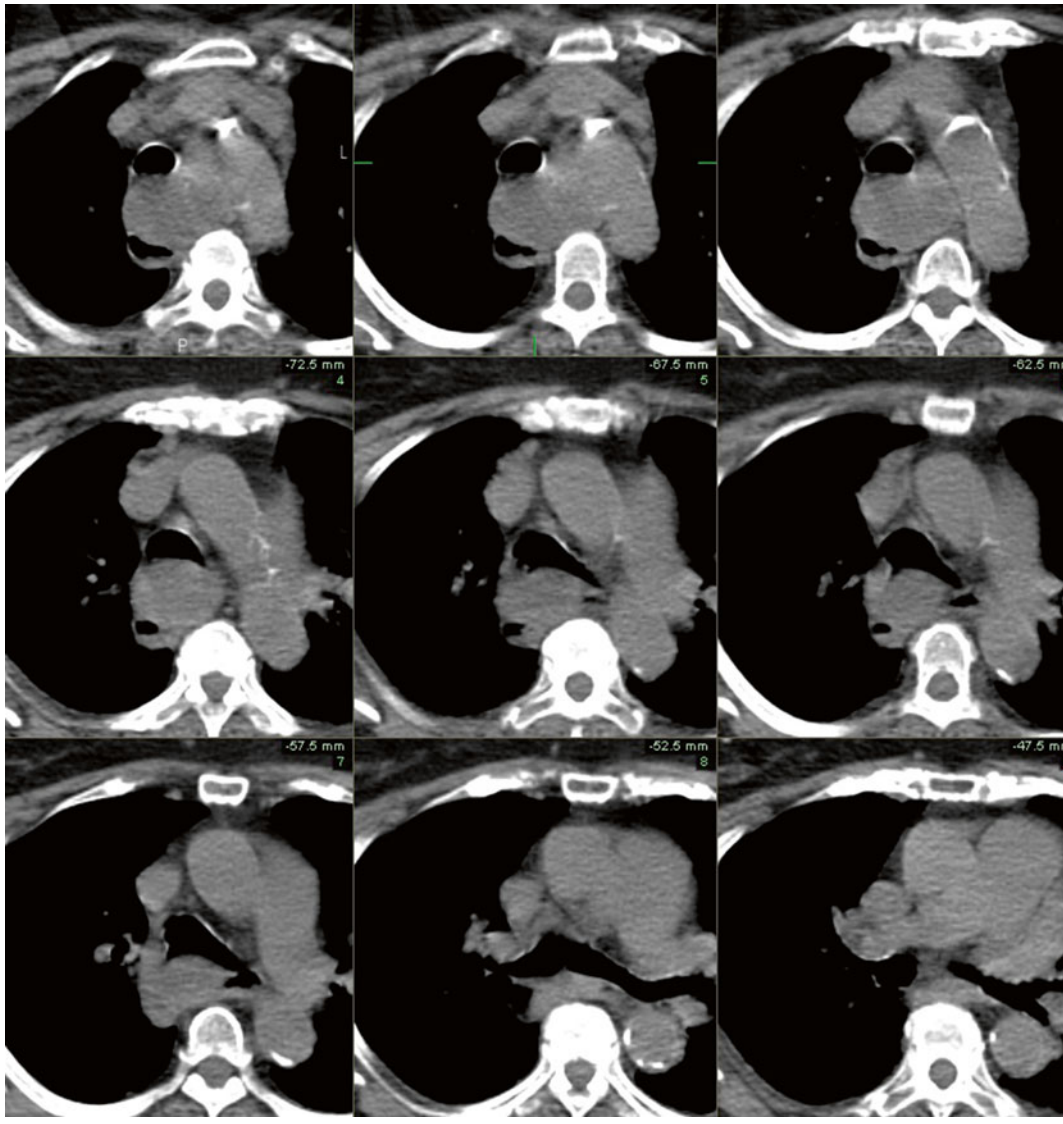

Fig. 15.19

Case 15.8

A 63-year-old male with hyperlipidemia, hypertension, and chest pain was referred for assessment of coronary artery disease. Spiculated left upper lobe mass on transmission scan (Fig. 15.20) was identified. The mass was pathologically confirmed following wedge resection as primary pulmonary neoplasm.

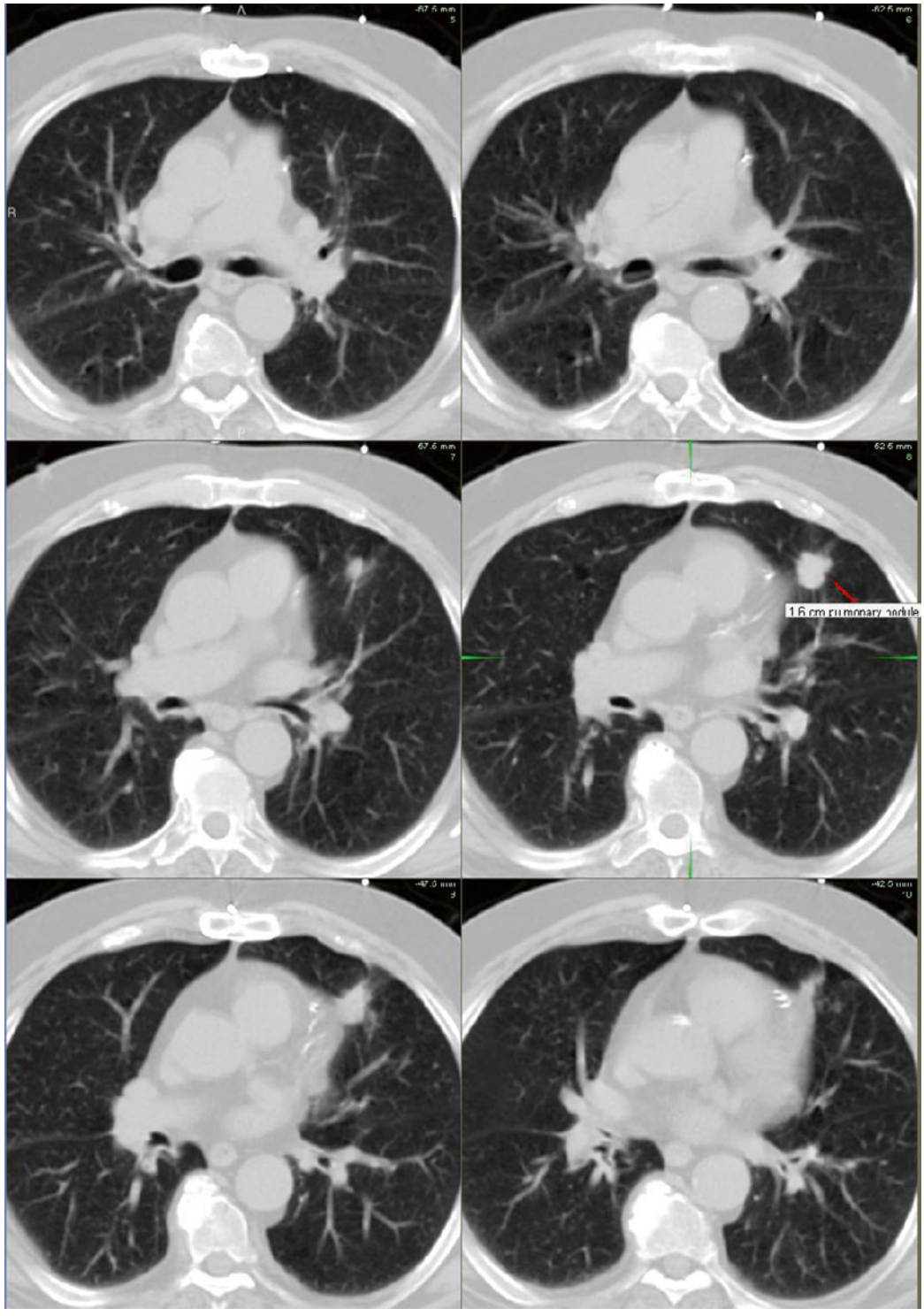

Fig. 15.20

Suggested Reading

Abraham A, Nihhol G, Williams KA, et al. F-18-FDG PET imaging of myocardial viability in an experienced center with access to F-18-FDG and integration with clinical management teams: the Ottawa-FIVE sub study of the PARR 2 Trial. J Nucl Med. 2010;51:567–74.

Bax JJ, Veening MA, Visser FC, et al. Optimal metabolic conditions during fluorine-18 fluorodeoxyglucose imaging: A comparative study using different protocols. Eur J Nucl Med. 1997;24:35–41.

Bax JJ, Visser FC, Poldermans D, et al. Feasibility, safety and image quality of cardiac FDG studies during hyperinsulinemic-euglycemic clamping. Eur J Nucl Med. 2002;29:452–7.

Brix G, Lechel U, Glatting G, et al. Radiation exposure of patients undergoing whole-body dual-modality F-18 PET/Ct examinations. J Nucl Med. 2005;46:608–13.

Brogsitter C, Gruning T, Weise R, et al. F-18-FDG PET for detecting myocardial viability: validation of 3D data acquisition. J Nucl Med. 2005;46:19–24.

Di Carli MF, Murthy VL. Cardiac PET/CT for the evaluation of known or suspected coronary artery disease. Radiographics. 2011;31(5):1239–54.

Eckerman KF, Endo A, editors. MIRD: radionuclide data and decay schemes. Reston: Society of Nuclear Medicine; 2008. p. 52.

Fukuchi K, Ohta H, Matsumura K, et al. Benign variations and incidental abnormalities of myocardial FDG uptake in the fasting state as encountered during routine oncology positron emission tomography studies. Br J Radiol. 2007;80(949):3–11. Epub 2006 Sep 27.

Go RT, Marwick TH, MacIntyre WJ, et al. A prospective comparison of rubidium-82 PET and thallium-201 SPECT myocardial perfusion imaging utilizing a single dipyridamole stress in the diagnosis of coronary artery disease. J Nucl Med. 1990;31:1899–905.

Hays MT, Watson EE, Thomas SR, et al. MIRD dose estimate report no. 19: radiation absorbed dose estimates from F-18-FDG. J Nucl Med. 2002;43:210–4.

Hernandez-Pampaloni M, Bax JJ, Morita K, et al. Incidence of stunned, hibernation and scarred myocardium in ischaemic cardiomyopathy. Eur J Nucl Med Mol Imaging. 2005;32:314–21.

Huitink JM, Visser FC, van Leeuwen GR, et al. Influence of high and low plasma insulin levels on the uptake of fluorine-18 fluorodeoxyglucose in myocardium and femoral muscle, assessed by planar imaging. Eur J Nucl Med. 1995;22:1141–8.

Langah R, Spicer K, Gebregzlabher M, et al. Effectiveness of prolonged fasting F-18-FDG PET-CT in the detection of cardiac sarcoidosis. J Nucl Cardiol. 2009;16:801–10.

Lehman SJ, Abbara S, Cury RC, et al. Significance of cardiac computed tomography incidental findings in acute chest pain. Am J Med. 2009;122(6):543–9.

Lewis P, Nunan T, Dynes A, et al. The use of low-dose intravenous insulin in myocardial F-18 FDG PET scanning. Clin Nucl Med. 1996;21:15–8.

Loghin C, Sdringola S, Gould KL. Common artifacts in PET myocardial perfusion images due to attenuation-emission misregistration: clinical significance, causes, and solutions. J Nucl Med. 2004;45(6):1029–39.

Martin WH, Jones RC, Delbeke D, et al. A simplified intravenous glucose loading protocol for fluorine-18-florodeoxyglucose cardiac single-photon emission tomography. Eur J Nucl Med. 1997;24:1291–7.

Martinez-Möller A, Souvatzoglou M, Navab N, et al. Artifacts from misaligned CT in cardiac perfusion PET/CT studies: frequency, effects, and potential solutions. J Nucl Med. 2007;48(2):188–93.

Matsunari I, Kanayama S, Yoneyama T, et al. Myocardial distribution of F-18-FDG and Tc-99m-sestamibi on dual-isotope simultaneous acquisition SPET compared with PET. Eur J Nucl Med. 2002;29:1357–64.

Mesotten L, Maes A, Van de Werf F, et al. PET radiopharmaceuticals used in viability studies in acute myocardial infarction: a literature survey. Eur J Nucl Med. 2002;29:3–6.

Metrard G, Girault S, Capitain O, et al. Uncommon breast tumor attenuation artifact on radionuclide ventriculography. Clin Nucl Med. 2008;33(4):288–9.
Mettler FA, Bhargavan M, Thomadsen BR, et al. Nuclear medicine exposure in the United states, 2005–2007: preliminary results. Semin Nucl Med. 2008;38:384–91.
Mirpour S, Khandani AH. Extracardiac abnormalities on rubidium-82 cardiac positron emission tomography/computed tomography. Nucl Med Commun. 2011;32(4):260–4.
Mueller J, Jeudy J, Poston R, et al. Cardiac CT angiography after coronary bypass surgery: prevalence of incidental findings. Am J Roentgenol. 2007;189(2):414–9.
Nye JA, Esteves F, Votaw JR. Minimizing artifacts resulting from respiratory and cardiac motion by optimization of the transmission scan in cardiac PET/CT. Med Phys. 2007;34(6):1901–6.
Sandler MP, Bax JJ, Patton JA, et al. Fluorine-18-fluorodeoxyglucose cardiac imaging using a modified scintillation camera. J Nucl Med. 1998;39:2035–43.
Schelbert HR. F-18-deoxyglucose and the assessment of myocardial viability. Sem Nucl Med. 2002;32:60–9.
Schinkel AFL, Bax JJ, Valkema R, et al. Effect of diabetes mellitus on myocardial F-18-FDG SPECT using acipimox for the assessment of myocardial viability. J Nucl Med. 2003;44:877–83.
Stankewicz MA, Mansouir CS, Eisner RL, et al. Myocardial viability assessment by PET: Rb-82 defect washout does not predict the results of metabolic-perfusion mismatch. J Nucl Med. 2005;46:1602–9.
Stewart RE, Schwaiger M, Molina E, et al. Comparison of rubidium-82 positron emission tomography and thallium-201 SPECT imaging for detection of coronary artery disease. Am J Cardiol. 1991;67:1303–10.
Stone CK, Holden JE, Stanley W, et al. Effect of nicotinic acid on exogenous myocardial glucose utilization. J Nucl Med. 1995;36:996–1002.
Van Campen CMC, Viser FC, van der Weerdt AP, et al. FDG PET as a predictor of response to resynchronization therapy in patients with ischaemic cardiomyopathy. Eur J Nucl Med Mol Imaging. 2007;34:309–15.
Waxman AD, Barondess P. Preparing patients for PET imaging: the importance of prescan communication. Discussion in PET Imaging. New York: CMP Healthcare Media; 2004.